Results in Engineering 8 (2020) 100168

Contents lists available at ScienceDirect

Results in Engineering

journal homepage: www.editorialmanager.com/rineng/Default.aspx

Non-linear finite-element investigation of the parameters affecting externally-bonded FRP flexural-strengthened RC beams

Ahmed Godat [a,*], Omar Chaallal [b], Yasmeen Obaidat [c]

[a] Department of Civil and Environmental Engineering, United Arab Emirates University, Al-Ain, B.O. Box 15551, United Arab Emirates
[b] Department of Construction Engineering, Université de Québec, École de Technologie Supérieure, Montréal, QC, H3C 1K3, Canada
[c] Department of Civil Engineering, Jordan University of Science and Technology, Irbid, 22110, Jordan

ARTICLE INFO

Keywords:
Flexural strengthening
Fibre-reinforced polymers (FRP)
Reinforced-concrete (RC) beams
Finite-element analysis
Parametric study
Flexural-strengthening schemes

ABSTRACT

This paper presents a three-dimensional non-linear finite-element model developed to simulate the behaviour of reinforced-concrete (RC) beams strengthened in flexure with carbon fibre-reinforced polymers (CFRP). The model is used to identify the parameters that have a significant influence on the behaviour of FRP flexural-strengthened beams. The parameters investigated are the width, length, thickness, and elastic modulus of the FRP laminate, as well as the number of FRP layers. The effect of two flexural-strengthening schemes is studied: a beam with two FRP plates at the soffit of the beam beneath the longitudinal steel, and a beam with a double layer of CFRP plates on the bottom face of the beam. The accuracy of the finite-element model is validated against published experimental data. Comparisons between numerical predictions and test results show very reasonable accuracy in terms of ultimate load-carrying capacities, load-deflection relationships, and failure modes. Results of the parametric study indicate that for some parameters, there is a threshold for the contribution of FRP laminates. The effect of the two flexural-strengthening schemes on the behaviour of FRP flexural-strengthened beams is also demonstrated.

1. Introduction

The strengthening of concrete structures by means of externally bonded (EB) fibre-reinforced polymers (FRP) is now routinely considered to be an effective method for enhancing the load-carrying capacity of existing structures. The large body of literature in the field of FRP rehabilitation, along with the corresponding increase in the level of activity, confirms the fact that these new materials are rapidly gaining wide acceptance by the civil engineering community [1,2]. The debonding problem remains the main disadvantage that reduces the efficiency of the EB strengthening technique because it prevents strengthened beams from attaining their full capacity.

When debonding failures occur, they usually result from shear failure of a thin layer of concrete adjacent to the adhesive. Adhesives currently used in FRP strengthening applications generally ensure that the bond strength of the adhesive is sufficient to transfer the interfacial stresses from the FRP to the concrete or vice versa. As a result, researchers have concluded that the bond strength of externally bonded FRP depends mainly on the quality of the surface preparation and the quality of the concrete itself, especially its shear strength. Unfortunately, due to the complexities of FRP/concrete interfacial behaviour, the numerical modelling of reinforced-concrete (RC) members flexural-strengthened with externally bonded (EB) fibre-reinforced polymers (FRP) has attracted less researchers during the last decade compared to experimental tests [3–12], although a considerable amount of experimental data has been published, e.g. Ashour et al. [13]; Pham and Al-Mahaidi [14]; Lundquist et al. [15]; Ai-Hui et al. [16]; Coronado and Lopez [17]; Li et al. [8]; Kotynia et al. [10]; Pannirselvam et al. [18]; and Ibrahim and Salman [11]. Finite-element models are useful for simulating FRP flexural-strengthened beams, which is a more economical approach than conducting laboratory tests. Previous finite element analysis research studies limited the use of their model to simulate their experimental data without performing parametric studies. Reinforced-concrete beams strengthened in flexure by externally bonded FRPs exhibit complex behaviour controlled by many parameters. An accurate finite-element model that represents the real behaviour of FRP flexural-strengthened beams and accounts for the various parameters would appear to be an effective tool for developing robust predictive equations that are useful for practical design work.

As a contribution to fill this need, a versatile numerical model has

* Corresponding author.
E-mail addresses: Ahmed.Godat@uaeu.ac.ae (A. Godat), Omar.Chaallal@etsmtl.ca (O. Chaallal), ytobeidat@just.edu.jo (Y. Obaidat).

https://doi.org/10.1016/j.rineng.2020.100168
Received 17 June 2020; Received in revised form 24 August 2020; Accepted 26 August 2020

been developed in this research to predict accurately the response of FRP flexural-strengthened beams. A three-dimensional finite-element model is developed using the ABAQUS finite-element package (2010). The proposed three-dimensional numerical model is applied to several cases of EB flexural-strengthened beams having various FRP strengthening configurations. The accuracy of the model is evaluated by comparing the numerical predictions with the experimental results. Once the accuracy of the model has been established, it is used to identify various parameters that strongly influence the behaviour of FRP flexural-strengthened beams. The significance of the present findings with respect to the various parameters is discussed.

2. Literature review and objectives

The literature review presented in this study covers the parameters that influence the behaviour of FRP flexural-strengthened beams as well as the numerical models developed to simulate the behaviour of such beams.

2.1. Literature on parameters of FRP flexural-strengthened beams

2.1.1. Number of layers

The number of FRP layers has a significant effect on the behaviour of FRP flexural-strengthened beams. It has been stated that increasing the number of FRP layers increases the beam capacity [19,20]. However, with more number of layers the mid-span deflection of beams decreases. Hooque [21] mentioned that the rate of load increase is appropriate to the increase in FRP layer number. David et al. [22] and Toutanji et al. [23] stated that the occurrence of debonding failure makes it no longer possible to increase the flexural capacity of the member by increasing the number of FRP layers.

2.1.2. FRP thickness

Similarly the effect that observed for the number of layers, increasing FRP thickness leads to accelerate the debonding failure [8,13,24–28]. Hu et al. [3]; Yang et al. [6]; Pannirselvam et al. [18] and Pathak [29] obtained a different conclusion, showing that flexural strength and stiffness increase with increasing the FRP thickness. The failure mode has been found to convert from plate-end debonding to intermediate-crack with increasing the FRP thickness [14]. The latter study showed that the load capacity increases with the FRP plate thickness up to a certain limit. Beyond this limit, further increase in FRP plate thickness did not lead to any increase in the flexure strength. This supports the conclusion that the interfacial stresses increase with FRP thickness and motivate debonding occurrence beyond a certain thickness. A study conducted by Shin and Lee [30] concluded that the FRP thickness does not have significant effect on the capacity of flexural-strengthened beams.

2.1.3. FRP elastic modulus

Increasing the FRP elastic modulus leads to increase interfacial stresses [25]. Rahimi and Hutchinson [24]; and Pathak [29] concluded that the characteristics of strengthened beams in terms of stiffness, load-carrying capacity, and mid-span deflection increased with the modulus of elasticity. However, the beam ductility at failure decreases with the increase of FRP elastic modulus [31]. Wu et al. [32] found that the use of high modulus carbon sheets increases the flexural stiffness, yielding load, ductility and reduces the crack propagation.

2.1.4. FRP length

A proportional relation between the FRP length and the load carrying capacity was stated by Fanning and Kelly [33]; Nguyen et al. [34]; Shin and Lee [30]; Yang et al. [6]; Ashour et al. [13]; Pham and Al-Mahaidi [14] and Hooque [21]. They declared that as the FRP plate length decreased, both the load-carrying capacity and the maximum deflection of the beam decreased. Li et al. [8] mentioned that crack propagation is related to the change of FRP plate length and results in the variation of failure mode of beams. Al-Tamimi et al. [27] specified a plate length of 25% of the beam length or more to avoid having the debonding failure. As well, they stated that the FRP length is the main reason of various FRP/concrete interfacial stresses in FRP flexural-strengthened beams. Hooque [21] stated that the increase of FRP length beyond 50% of the beam length does not add significant contribution to the load-carrying capacity and the mid-span deflection. It should be noted that the ACI 440.2 (2014) provides general guidelines instead of detailed analysis for the location of cuttoff points to prevent the debonding.

2.1.5. FRP width

The influence of the FRP to the behaviour of FRP flexural-strengthened beams was only studied by Lu et al. [35] and Hind et al. [28]. They observed that an increase in FRP width leads to increase the capacity of flexural-strengthened beam. In addition, it was stated that large FRP width concentrate the failure at the FRP/concrete layer [28]. The FRP strip-to-concrete width ratio is adopted from the FRP-to-concrete pull-out tests. It has been shown that the bond stresses from the FRP laminate to the concrete increases for low width of FRP plate [4].

2.1.6. Strengthening scheme

The arrangement of FRP laminates at the soffit of the beam beneath the longitudinal steel provides greater strengthening capacity compared to the traditional flexural-strengthening scheme [36]. Brena et al. [37] tried to strengthen beams with FRP plates located on the sides of the beam parallel to the longitudinal steel. They found that this strengthening method delayed, or in some cases prevented, the debonding, especially when adding transverse FRP strips along the shear span. In another study, Brena and Macri [38] concluded that specimens with configurations involving a larger contact surface with equal areas of composite materials were capable of reaching higher stresses as a result of larger deformation capacities and lower interface shear stresses.

Based on a review of the parameters influencing the behaviour of FRP flexural-strengthened beams, it appears that the effect of the parameters are somewhat contradictory and to a certain degree controversial. To the authors' knowledge, there is no study in the literature that has investigated these parameters in one study. In addition, many aspects have still not been fully verified due to the relatively large scatter observed in research studies.

2.2. Literature review on finite-element models

Various constitutive laws have been used to simulate FRP flexural-strengthened beams. In early models, linear elastic analyses were implemented, while the recent trend has been directed towards the use of non-linear finite-element models. A review of past studies on the application of finite-element analysis to model FRP flexural-strengthened RC beams is presented here. A description of concrete constitutive laws and various techniques for modelling FRP strengthening materials is given. A special attention is placed on the different techniques that have been incorporated in finite-element analyses to simulate the FRP/concrete interfacial behaviour.

2.2.1. Concrete constitutive law

Various constitutive laws have been adopted in the simulations of FRP flexural-strengthened beams. These models include non-linear elastic models [5,9,10,14,19,35,39–43] and plasticity-based models, whether perfect plasticity models [11,21,28,44–52] or elastic-plastic models [29,39,53–57]. The failure of concrete under a general state of stress has been represented using a two-parameter criterion, such as the Drucker-Prager [32] or Mohr-Coulomb criteria [3]. In addition, a five-parameter model has also been used to represent the failure surface of concrete [8]. To date, damage models have been rarely used to simulate concrete non-linearities; only the Rahimi and Hutchinson [24] and Abdel-Baky [42] FE models included an isotropic damage model for concrete.

Previous elasticity or plasticity concrete relations have been successfully used to represent load non-linearities (load-deflection behaviour of flexurally strengthened beams). This is possible because the flexural responses of the strengthened beams depend mainly on the tensile and cracking behaviour of the concrete rather than on the compressive behaviour. Marvila et al. [58] investigated the effect of excess materials on the mortar strength. It has been found that the there is no change in strength properties of mortar when destructive test and finite element modelling results were compared.

2.2.2. FRP/concrete interface

Abundant amount of researchers have been carried finite element analysis of FRP flexural-strengthened beams without considering the FRP/concrete interfacial behaviour. To correctly simulate debonding of the FRP/concrete interface, elements having a predefined bond-slip relation are used to link the FRP and the concrete nodes [10,29,35,39–42,53–55]. These interface elements have no physical dimensions. In addition, the debonding load can in several cases be predicted using such interface elements or using a predefined discrete-crack model.

Few studies have been presented using a non-linear fracture mechanics-based discrete-crack analysis to investigate the interaction of bond properties on the performance of flexural-strengthened beams [6,9,14,59]. Niu and Wu [40] investigated the interaction between concrete cracking and the behaviour at FRP/concrete interfaces. The study concluded that the characteristics of the bond-slip model in terms of the bond strength and the initial slope of the curve have a negligible effect on the load-deflection behaviour of FRP flexural-strengthened beams. However, the fracture energy of the bond-slip relationship has a significant effect on the debonding load [60].

2.2.3. Concrete/longitudinal steel interface

The finite-element models used to account for steel/concrete interfacial behaviour have used either a bilinear bond-slip model [5] or an elastic-plastic model [32,39,40] to represent the steel/concrete interface. Although interface elements have been extensively used to represent FRP/concrete interfaces, most studies have ignored the bond-slip behaviour between the steel reinforcement and the concrete. This has been justified by the fact that the reduction in structural stiffness arising from the relative slip between the steel reinforcement and the concrete can generally be included in the tension stiffening model of the concrete. Some models attempted to represent the tension stiffening effect by increasing or decreasing the stiffness of the cracked concrete. On the other hand, introducing relative slip between reinforcement bars and surrounding concrete elements reduces the overall stiffness of the structure.

2.2.4. Modelling of bonded FRP plates

Generally, two approaches have been used to represent the behaviour of bonded FRP plates in flexural-strengthened concrete beams. The first approach involves converting the FRP plates to equivalent truss elements. This approach is attractive because of its simplicity [8,9,35,39] and is used in two-dimensional models. The area of the truss element is equivalent to that of the FRP composites. In the second approach, shell elements are used [3,10,28,51,56]. With these elements, the out-of-plane stresses are considered to be negligible. A failure criterion must also be defined to describe FRP rupture under general plane stress conditions. Such criteria must account for the orthotropic nature of the FRP plates.

2.3. Objectives

The specific objectives of this study are: (a) investigate the effectiveness of various parameters reported in the literature to affect the performance of FRP flexural-strengthened beams; (b) study the methodology of previously developed finite element models to simulate the behaviour of FRP flexural-strengthened beams; (c) develop a finite element model to clarify the various conflicting parameters that strongly influence the behaviour of FRP flexural-strengthened beams, such as FRP width, length, thickness, elastic modulus and number of FRP layers; and (d) compare the effectiveness of two strengthening schemes widely used in practice: a beam with two FRP plates at the soffit of the beam beneath the longitudinal steel, and a beam with a double layer of FRP plates on the bottom face of the beam.

3. FINITE-ELEMENT model

A three-dimensional finite-element model is developed to simulate accurately the behaviour of FRP flexural-strengthened beams. The initial phase of the numerical study involves the development of an accurate finite-element model to simulate the control (unstrengthened) RC beam. The quality of this model is assessed by comparing numerical results with experimental data. In the second phase of the numerical study, the control-beam model is modified to accommodate the presence of external FRP composites for flexural strengthening. The accuracy of this model is again measured by comparing its predictions with experimental data. The goal of these phases is to ensure that the numerical model captures the actual behaviour of tested beams. A flow chart of typical phases of finite element model development is presented in Fig. 1.

3.1. Material modelling

3.1.1. Concrete

The constitutive model used for the concrete corresponds to that provided in the ABAQUS [61] software. A brief description of the main features of the model is presented in this paper. The damaged-concrete plasticity model in ABAQUS [61] provides a general capability for modelling concrete in all types of structures, including beams, trusses, shells, and solids. The concrete model provides the capability to simulate cracking for reinforced concrete elements using one of the three crack models, namely: (i) smeared crack concrete model; (ii) brittle crack concrete model; and (iii) concrete damaged plasticity model. In this study, the concrete damaged plasticity model is employed to represent the inelastic behaviour of concrete both in tension and compression including the damage characteristics. This model was selected for its capability to simulate the concrete under any loading combinations. In this model, the evolution of the yield (or failure) surface is linked to failure mechanisms under tension and compression loading. It assumes that the uniaxial stress-strain curves are converted into stress versus plastic-strain curves. It combines three features to simulate the basic characteristics of concrete. These features include a plasticity-based rules and damage ingredients to accommodate the strain-softening behaviour of the material under increasing compressive stresses. In addition, a failure criterion for concrete is used to define the cracking stress in tension and the failure envelope in compression. The failure envelope accounts for multi-axial stress conditions.

The tensile behaviour of concrete takes into account cracking, shear modulus degradation, fracture energy, and tension stiffening. Tension stiffening is modelled as a linearly descending branch in the stress-strain relationship after the peak point at which the concrete cracks is reached, as shown in Fig. 2. The two descending branches of the tensile stress-strain curve (Fig. 2) are considered to accurately capture the response by primary and secondary cracks. For the finite-element implementation, the values of the compressive strength $\hat{f}_c$ (MPa) were taken from the relevant set of experimental data. The tensile strength f_t (MPa), and the elastic modulus E_c (MPa) were approximated based on the following [62,63] equations:

$$f_t = 0.35\sqrt{f_c'} \tag{1}$$

$$E_c = 4700\sqrt{f_c'} \tag{2}$$

The inelastic parameter associated with the softening part of the

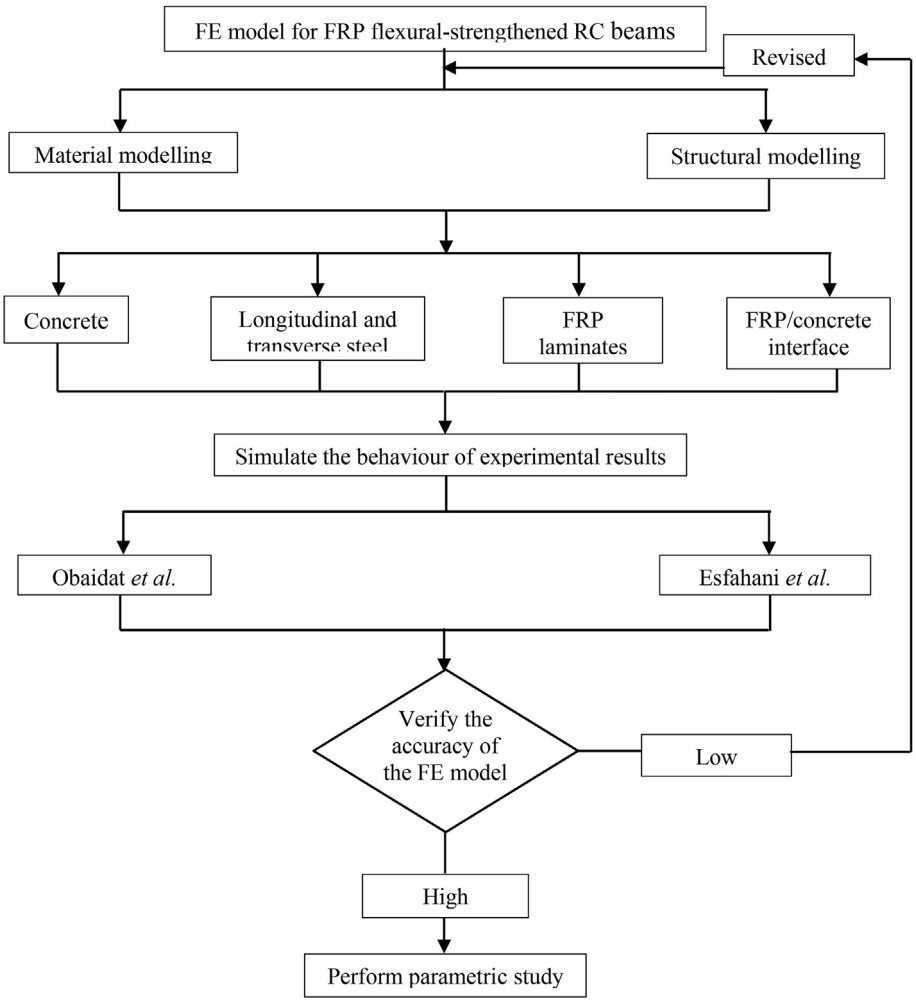

Fig. 1. Typical phases of finite element model development.

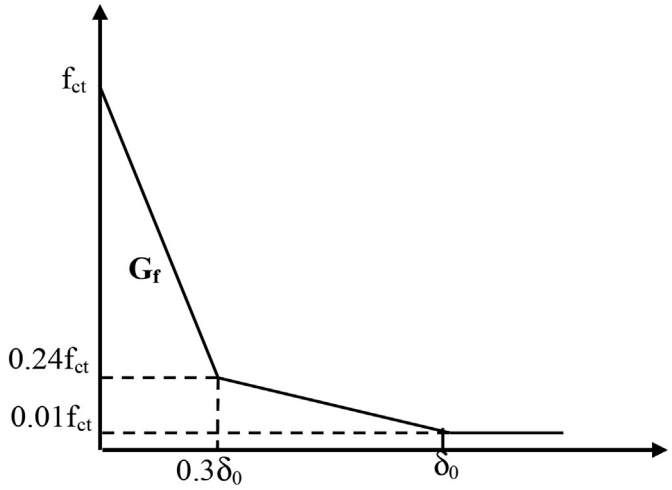

Fig. 2. Softening curve of concrete under uniaxial tension.

curve is the fracture energy (G_f). The fracture energy for mode I is the area under the softening curve and can be estimated as follows [64]:

$$G_f = G_{f0}\left(\frac{f_c^{'}}{10}\right) \tag{3}$$

where G_{f0} is a constant determined based on the maximum aggregate size d_{max}. Then the crack opening is calculated from the fracture energy, as shown in Fig. 2.

Under uniaxial compression, the response is linear up to the initial value, σ_{co}, which is 50% of the ultimate compressive stress, σ_{cu}. In the plastic regime, the response is typically characterized by stress hardening followed by strain softening beyond the ultimate compressive stress. In the concrete model, the stress-strain relationship proposed by Saenz [65] was used to represent the uniaxial compressive stress-strain curve for concrete and has the following form:

$$\sigma_c = \frac{E_c\varepsilon_c}{1 + (R + R_E - 2)\left(\frac{\varepsilon_c}{\varepsilon_0}\right) - (2R - 1)\left(\frac{\varepsilon_c}{\varepsilon_0}\right)^2 + R\left(\frac{\varepsilon_c}{\varepsilon_0}\right)^3} \tag{4}$$

$$R = \frac{R_E(R_\sigma - 1)}{(R_\varepsilon - 1)^2} - \frac{1}{R_\varepsilon} \tag{5}$$

$$E_0 = \frac{f_c^{'}}{\varepsilon_0} \tag{6}$$

$$R_E = \frac{E_c}{E_0} \tag{7}$$

where $R_E = 4$; and $R_\sigma = 4$, as reported in Hu and Schnobrich [66].

The concrete damaged plasticity model uses factors that characterise the degradation of concrete with the increase of applied load. When the

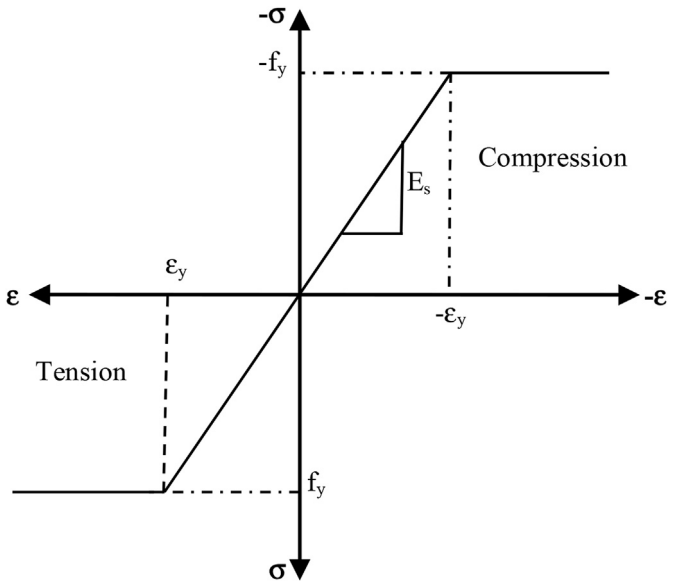

Fig. 3. Stress-strain curve for steel reinforcement.

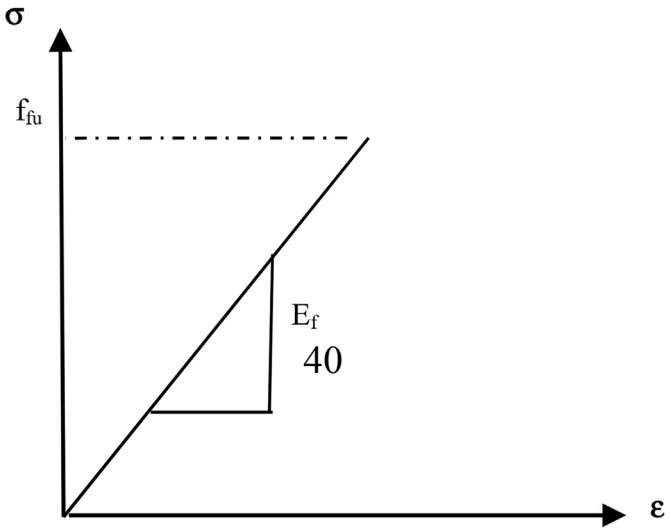

Fig. 4. Stress-strain curve for unidirectional CFRP composite.

concrete specimen is unloaded from any point on the strain softening branch of the stress-strain curves, the unloading response is weakened: the elastic stiffness of the material appears to be degraded (or damaged). The factors used are w_c and w_t to represent the compressive stiffness recovery and the tensile stiffness recovery, respectively. This study uses $w_c = 1.0$ and $w_t = 0$, representative of full compression recovery and lack of tension recovery. The value of $w_c = 1.0$ is adequate for quasi brittle materials [67]. The degradation of the elastic stiffness is characterized by two damage variables, d_c and d_t, which are the ratio of inelastic strain to total strain, and ratio of cracking strain to the total strain, respectively. These variables are functions of the plastic strains, temperature, and field variables. The damage variables can take values from zero, representing the undamaged material, to one, which represents total loss of strength. Poisson's ratio for concrete was taken as 0.2 for the beams considered.

3.1.2. *Steel reinforcement, steel loading plates and FRP*

As shown in Fig. 3, the steel reinforcement was represented by an elastic-plastic constitutive relation with linear strain hardening. A linear elastic tensile model until failure was assumed to simulate the FRP laminates and steel loading plates. The rupture point on the stress-strain relationship defines the maximum stress and strain of the FRP composites (Fig. 4).

3.2. *Structural modelling*

In this analysis, appropriate geometrical elements were used to represent the behaviour of the concrete, the steel reinforcement and the FRP laminates. A four-node linear tetrahedral element with three degrees of freedom at each node was used to describe the behaviour of the concrete, steel and FRP. Such elements satisfy shear and bending deformations. The element was characterized by plastic deformation, cracking in three orthogonal directions. A perfect bond between the steel reinforcement and the concrete was assumed. Ideally, the bond strength between the concrete and the steel reinforcements should also be considered. However, in the current application, the elements representing the longitudinal steel and the steel stirrups were directly connected to the concrete elements because no debonding was observed between these components in the experimental tests. Effects associated with the rebar/concrete interface, such as bond slip and dowel action, were modelled approximately by introducing the fracture energy into the concrete behaviour. Full strain compatibility was assumed between the FRP and the concrete because the FRP laminates remained well attached to the concrete until the end of the test, with failure being observed in the concrete substrate between the FRP and the longitudinal steel. An appropriate mesh size was used to capture this performance.

In the present study, the FRP/concrete interfacial behaviour is simulated by modelling the cracking and failure of the concrete elements located between the longitudinal steel and the FRP/concrete contact surface. This approach, referred to as the meso-scale model, is very effective as it uses a very fine mesh with element sizes of 0.45 mm, which is one order smaller than the thickness of the concrete debonding layer (45 mm). The advantage of this approach is that it models the thin concrete substrate adhering to the FRP, where the debonding initiates, leading thereby to an accurate model and capture the FRP/concrete interfacial responses [35]. In the meso-scale model, the influence of the interfacial normal stress components on the shear stress behaviour is disregarded to simulate the cracked concrete.

The non-linear load-deformation behaviour of the structure was simulated under displacement-controlled loading conditions, as was the case for the laboratory experiments. In view of the geometrical and loading symmetries, only one-quarter of the beam was simulated, as shown in Fig. 5. Sensitivity analysis was performed for finite element modelling of specimens in order to optimize the mesh size and the number of nodes per element. A convergence of results is obtained when an adequate number of elements and nodes are used in the model. This is achieved practically when an increase in the mesh density has a negligible effect on the results. Therefore, in the current research, a sensitivity analysis is carried out to specify an appropriate mesh density and to ensure that the spatial discretization used does not introduce excessive approximations into the simulations and to solve the problems related to regularization issues.

4. Experimental program

The proposed three-dimensional analysis is applied to various cases with different FRP strengthening configurations. These cases were selected for numerical analysis to cover a wide spectrum of FRP strengthening properties. These include beams strengthened with various FRP widths, lengths, and numbers of layers. The experimental tests used to validate the finite-element model are described by Obaidat et al. [68] and Esfahani et al. [69]. A brief description of the materials, strengthening technique, and test setup is presented here. A complete description of the experimental program is provided in the corresponding references. Table 1 lists the material properties, whereas Table 2 provides the geometrical characteristics and strengthening details of the various specimens.

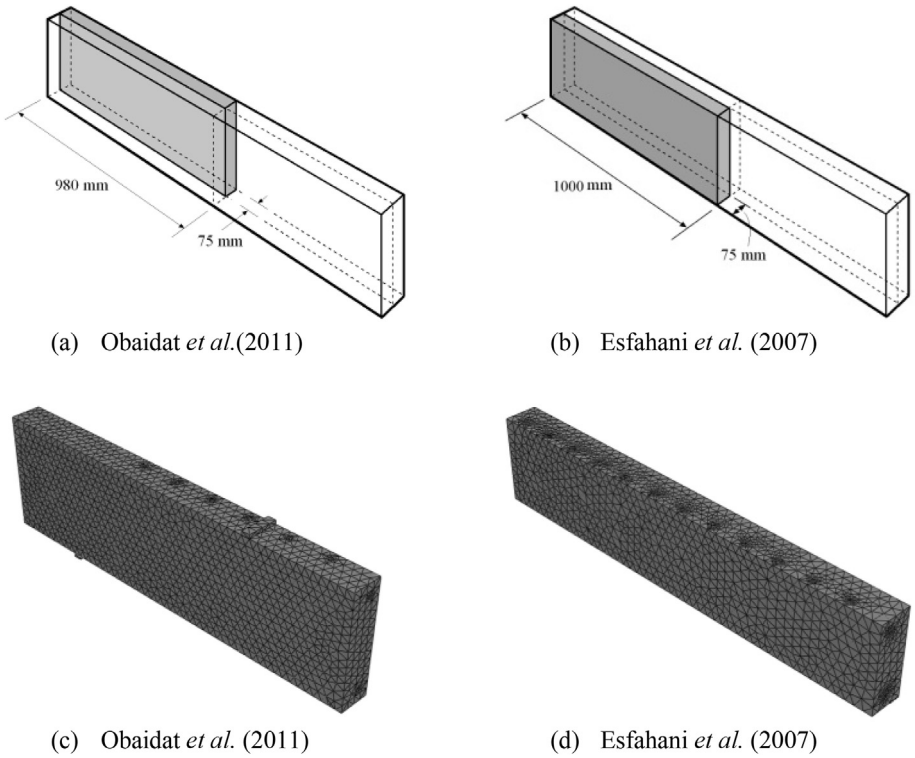

(a) Obaidat *et al.*(2011) (b) Esfahani *et al.* (2007)

(c) Obaidat *et al.* (2011) (d) Esfahani *et al.* (2007)

Fig. 5. Finite-element models.

Table 1
Mechanical properties of tested specimens.

			Obaidat et al. [68]	Esfahani et al. [69]
Steel	Steel 8	*fy* (MPa)	507	350
	Steel 10	*fy* (MPa)	507	365
	Steel 12	*fy* (MPa)	507	400
	E	(GPa)	210	210
	ν		0.3	0.3
Concrete	$f`_c$	(MPa)	30	25
CFRP	*E*	(GPa)	165	237
	f_{fu}	(MPa)	2000	2845

Table 2
CFRP strengthening details of tested specimens.

		CFRP Width (mm)	CFRP Thickness (mm)	CFRP Length (mm)	No. of CFRP Layers
Obaidat et al. [68]	CON	0	0	0	0
	RB1	50	1.2	1560	1
	RB2	50	1.2	1040	1
	RB3	50	1.2	520	1
Esfahani et al. [69]	B1-12D-0L	0	0	0	0
	B2-12D-1L15	150	0.176	1400	1
	B3-12D-2L15	150	0.176	1400	2
	B4-12D-3L15	150	0.176	1400	3

4.1. Obaidat et al. Specimens

For the specimens analyzed by Obaidat et al. [68]; the experimental program involved four tests performed on RC rectangular-section beams with a total length of 1960 mm. The control specimen, which was not strengthened with carbon FRP plates, was labelled CON, whereas the specimens retrofitted using the CFRP plates were labelled RB, as shown in Table 2. Specimen RB1 had a CFRP length of 1560 mm, while specimens RB2 and RB3 had CFRP lengths of 1040 and 520 mm, respectively. The arrangement of the longitudinal steel as well as the steel stirrups was identical in the four specimens, as shown in Fig. 6(a). The rectangular section had overall dimensions of 150 mm (width) by 300 mm (total depth). The shear span was 520 mm, and the effective depth was 270 mm.

The average concrete strength was 30 MPa. The internal flexural steel and the steel stirrups had a nominal yield strength of 507 MPa. The strengthening material was a unidirectional carbon plate with a nominal thickness and width of 1.2 mm and 50 mm, respectively, (area of 60 mm^2). The tensile strength and modulus of elasticity of the CFRP plates were 2000 MPa and 165 GPa, respectively. A commercially available epoxy paste was used to bond the CFRP plates to the concrete. The strengthened specimens were pre-cracked before strengthening. The strengthened specimens were precracked before the application of CFRP plates.

4.2. Esfahani et al. Specimens

The experimental results reported by Esfahani et al. [69] were also included in this study. They involved four specimens of RC rectangular-section beams with a total length of 2000 mm. The nominal shear span-to-depth ratio (a/d) was 3.5 for all beams. The dimensions and cross-sectional details of the test girders are presented in Fig. 5(b). The beams were heavily reinforced in shear to ensure that they would fail in bending. The experimental program included a control specimen labelled as B1-12D-0L, whereas the specimens retrofitted with CFRP sheets were labelled as B2-12D-1L, B3-12D-2L15, and B4-12D-3L15 to represent the first, second, and third strengthened specimens, respectively, as shown in Table 2. The specimens bonded with CFRP were strengthened with a single layer, double layers, and triple layers, with the length of the CFRP sheets being identical for all specimens. The ratio of

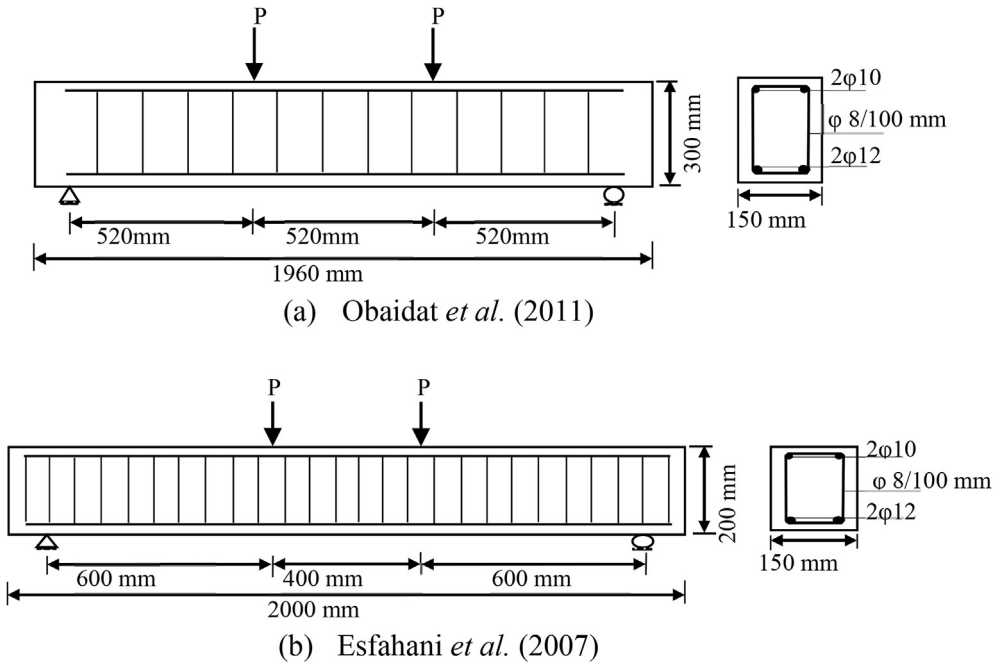

Fig. 6. Geometry, arrangement of reinforcement, and load location of tested beams.

the shear span-to-effective depth ratio (a/d) was constant for all specimens (3.87).

The average measured cylinder compressive strength obtained was 25 MPa. The yield stresses for Φ12, Φ10 and Φ8 bars were 400 MPa, 365 MPa, and 350 MPa, respectively. Unidirectional CFRP sheets with 0.176 mm thickness were used in this investigation. The CFRP sheets were characterized by high strength and high elastic modulus. The manufacturer reported an ultimate tensile strength of 2845 MPa and an elastic modulus of 237 GPa. The stress-strain relationship was essentially linear up to failure. To achieve maximum bonding, an epoxy adhesive was used to attach the fabric to the beam.

5. Numerical results and DISCUSSION

The accuracy of the numerical model is evaluated by comparing the numerical predictions to experimental results. Then, having verified the accuracy, parametric analyses are performed to gain a better insight into the parameters governing the behaviour of FRP flexural-strengthened beams.

5.1. Ultimate load-carrying capacity and failure modes

The primary objective of the numerical investigations is to establish the ability of the proposed analysis to simulate the behaviour of FRP flexural-strengthened beams. Various flexural strengthening configurations are considered to investigate the accuracy of the numerical model. The specimens considered in this study covers various ranges of strengthening strategies, geometric properties, and material properties. The cases analyzed involved eight specimens, corresponding to the specimens tested by Esfahani et al. [69] and Obaidat et al. [68].

The numerical model used to simulate the experimental beams proves to be capable of modelling correctly general trends and behaviour with very good accuracy for a wide variety of FRP flexural-strengthening applications, as shown in Fig. 7. The results shown in the figure indicate that the proposed numerical model is able to predict the ultimate load-carrying capacity with an average and a statistical deviation of 107% and 5.7%, respectively. Table 3 shows a comparison between experimental and numerical results. Generally, the numerical model predicts a higher load-carrying capacity than that obtained experimentally. This

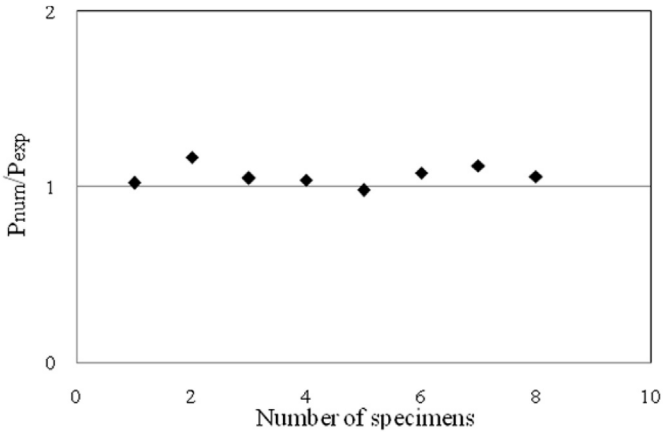

Fig. 7. Accuracy of numerical model versus experimental results.

Table 3
Comparison between experimental and numerical results.

Specimen	Experimental ultimate load (kN)	Numerical ultimate load (kN)	P_{num}/P_{exp}	Exp. Failure mode	Num. Failure mode
CON	122	125	1.02	Concrete crushing	Concrete crushing
RB1	161	189	1.17	CFRP debonding	CFRP debonding
RB2	133	139	1.05	CFRP debonding	CFRP debonding
RB3	127	132	1.04	CFRP debonding	CFRP debonding
B1-12D-0L	61	60	0.98	Concrete crushing	Concrete crushing
B2-12D-1L15	62	67	1.08	CFRP rupture	CFRP debonding
B3-12D-2L15	73	82	1.12	CFRP debonding	CFRP debonding
B4-12D-3L15	78	83	1.06	CFRP debonding	CFRP debonding

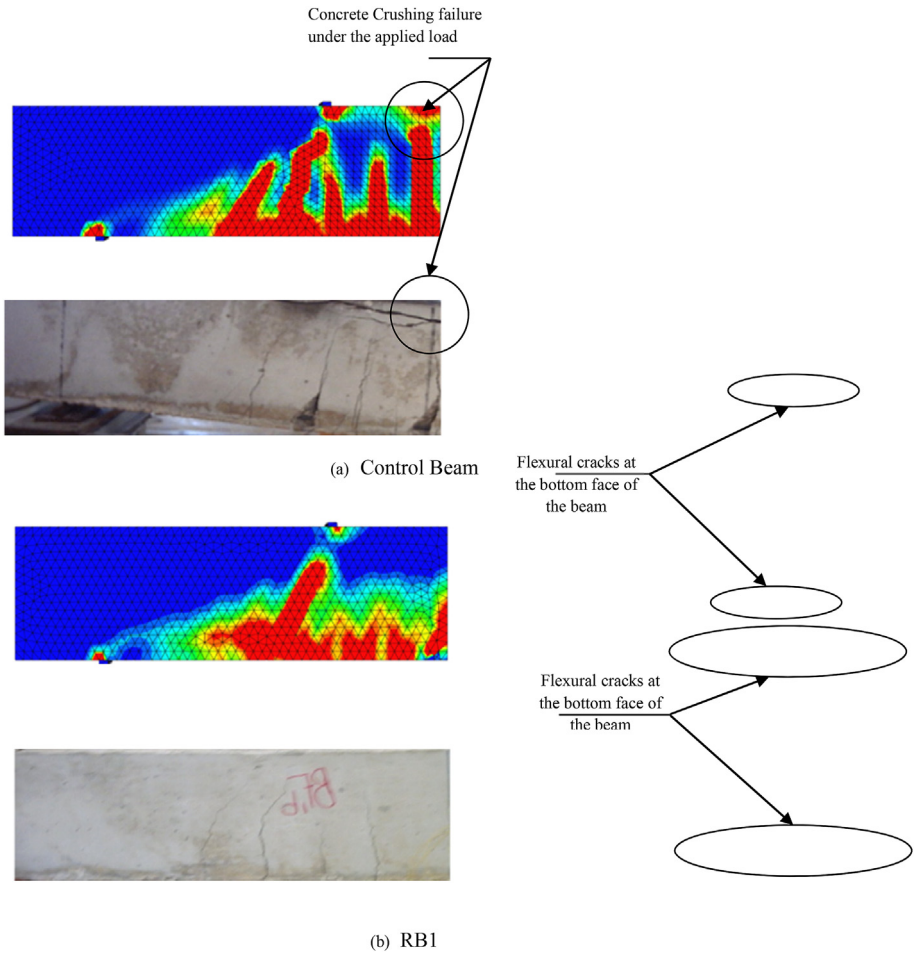

Fig. 8. Comparison between numerical and experimental results for load-deflection relationships.

can be attributed to the assumption of a full-contact bond between the longitudinal steel and the concrete. The numerical model can simulate failure modes identical to those observed experimentally. The position of the flexural cracks corresponds to experimental observations, as shown in Fig. 8.

Fig. 9 shows the load-deflection curves for the control beams and the strengthened beams. As it can be observed, the numerical model shows very good agreement with experimental results. It is clear that there is a small discrepancy between the stiffness of the experimental curves and numerical predictions. For the strengthened specimens, the numerical model does not accurately describe the post-peak behaviour. The numerical predictions of the maximum deflections differ from experimental observations.

5.2. Parametric study

The effect of important parameters such as the width, thickness elastic modulus and length of the FRP laminates as presented in Figs. 10–13 respectively, as well as the number of FRP layers, is investigated through a parametric study. The effect of two strengthening schemes for flexure is studied: a beam with two CFRP plates at the soffit of the beam beneath the longitudinal steel, and a beam with a double layer of CFRP plates. The parametric study is carried out for the two sets of beams described earlier, and the variations in ultimate load capacity and load-deflection relationship are used as a basis for comparison. The numerical results represent the deflection at the mid-span of the beam. The authors favour the ultimate load capacity because it is the key factor that determines the FRP flexural contribution. It can be mentioned that the analyses are stopped when FRP debonding occurred and that is the governing failure mode. For the two sets of beams, Table 4 details the variables along with their ranges of interest. Various ranges of each of these parameters are considered.

5.2.1. Effect of FRP width

The width ratio between the bonded plates and the concrete member has shown to have a significant effect on the ultimate bond strength [4]. In this study, various widths of FRP, ranging between 40 and 150 mm, are investigated. The 150-mm width covers the whole width of the beam. The numerical predictions show that the ultimate load-carrying capacity and mid-span deflection increase proportionally to the increase in FRP width (Fig. 10). This can be explained by the fact that an increase in FRP width proportionally leads to uniform transfer between the FRP and the concrete, which in turn delays debonding and increases ultimate load capacity.

To further investigate the influence of FRP width on the behaviour, the load-carrying capacities obtained for various ranges of FRP widths are plotted against the percentage increase in load capacity in Fig. 14. The loading-capacity plot in the figure corresponds to the peak force before descending. It can be seen that the greater the FRP width, the higher is the load capacity. The increase in FRP width from 40 to 150 mm is almost four times, while the load capacity increases to 3.6 times that of the specimen with low FRP width (40 mm). This confirms the effect of FRP width on FRP flexural-strengthened beams.

5.2.2. Effect of FRP thickness

The considerable effect of plate thickness on the behaviour of FRP flexural-strengthened beams is verified in this study. This variation is examined for different plate thicknesses: 0.176 mm, 0.33 mm, 0.501 mm,

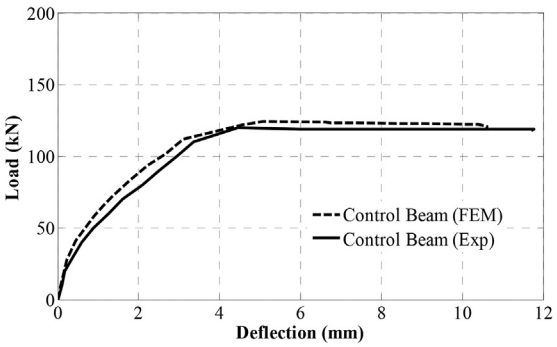

(a) Control Beam, Obaidat *et al.* (2011)

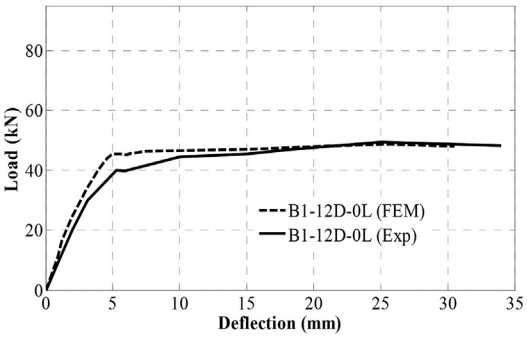

(b) B1-12D-0L, Esfahani *et al.* (2007)

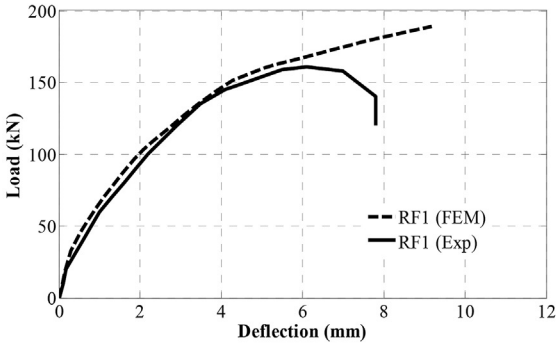

(c) RB1, Obaidat *et al.* (2011)

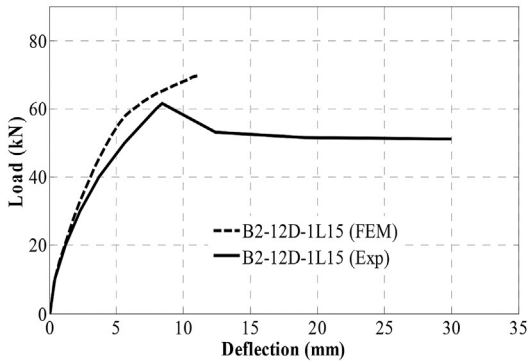

(d) B2-12D-1L15, Esfahani *et al.* (2007)

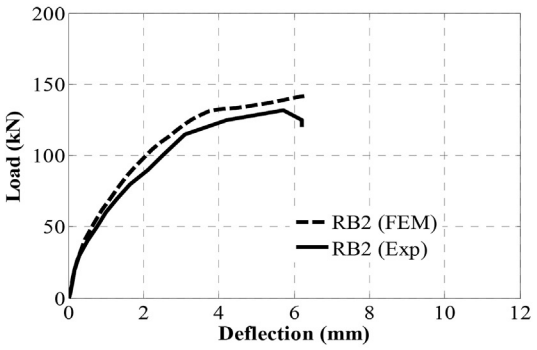

(e) RB2, Obaidat *et al.* (2011)

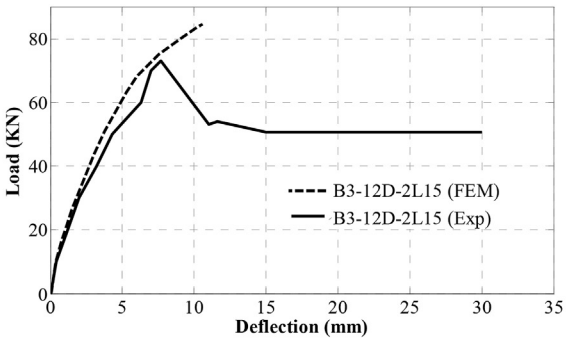

(f) B3-12D-2L15, Esfahani *et al.* (2007)

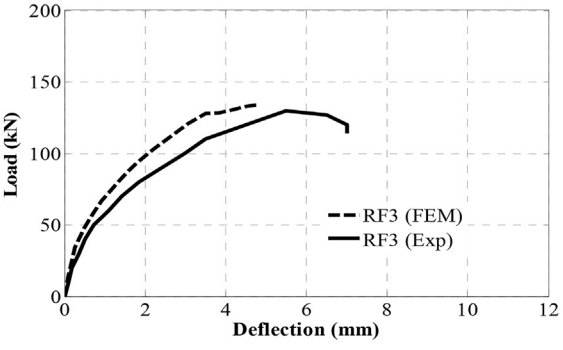

(g) RB3, Obaidat *et al.* (2011)

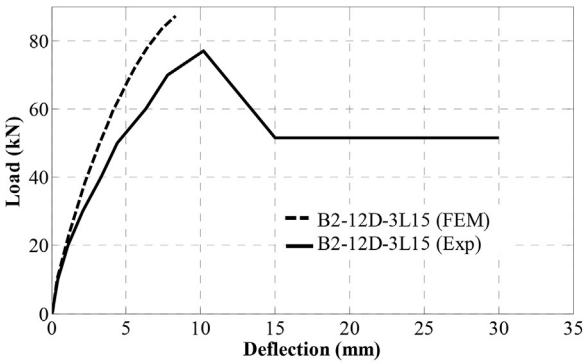

(h) B4-12D-3L15, Esfahani *et al.* (2007)

Fig. 9. Comparison between numerical and experimental failure modes.

1 mm, 1.2 mm, and 1.4 mm. As shown in Fig. 11, the increase in FRP thickness increases its contribution up to a certain level (1 mm). From Fig. 14, it can be observed that the beam capacity decreases with increasing the FRP thickness beyond 1 mm for the second set of specimens. This can be attributed to the fact that increasing the FRP thickness accelerates the FRP debonding. It indicates that the optimum FRP thickness is 1 mm for these cases, beyond which no increase in the load capacity is reported. The result presented here constitutes an upper

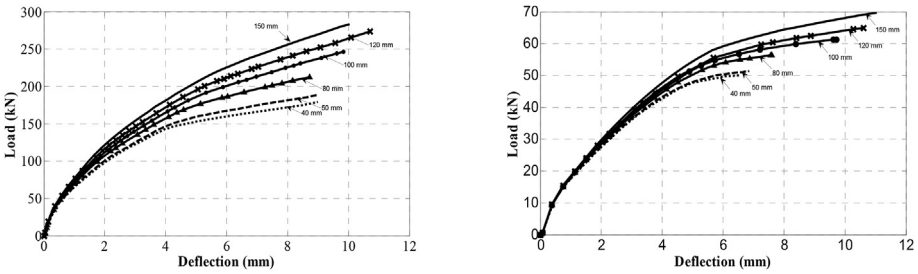

(a) Obaidat *et al.* (2011) (b) Esfahani *et al.* (2007)

Fig. 10. Load-deflection relationship for the FRP width effect.

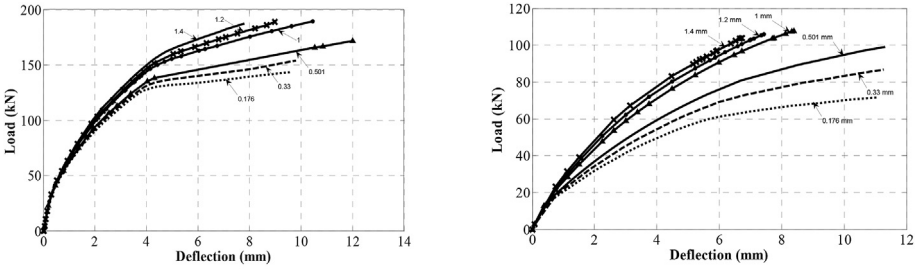

(a) Obaidat *et al.* (2011) (b) Esfahani *et al.* (2007)

Fig. 11. Load-deflection relationship for the FRP thickness effect.

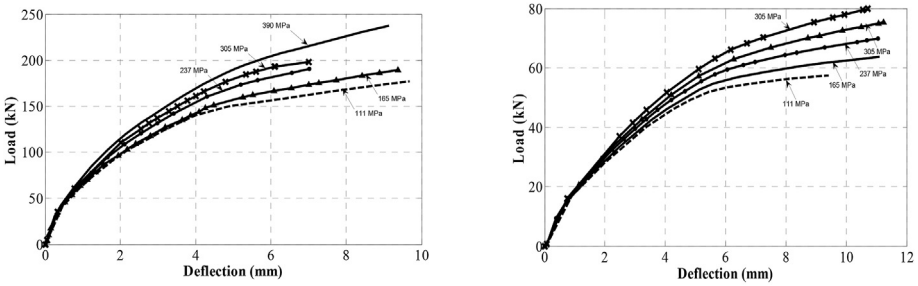

(a) Obaidat *et al.* (2011) (b) Esfahani *et al.* (2007)

Fig. 12. Load-deflection relationship for the FRP elastic modulus effect.

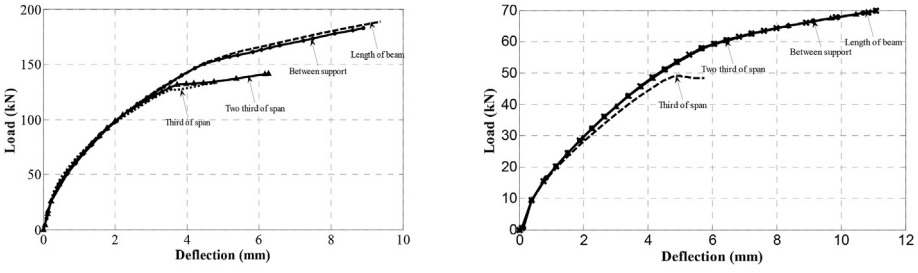

(a) Obaidat *et al.* (2011) (b) Esfahani *et al.* (2007)

Fig. 13. Load-deflection relationship for the FRP length effect.

bound for the impact of FRP thickness on FRP contribution, as mentioned in Pham and Al-Mahaidi [14]. It worth to mention that the beam ductility at failure decreases with the increase of FRP thickness although of the stiffness increase.

5.2.3. *Effect of FRP elastic modulus*

Various values of FRP elastic modulus are used to investigate the influence of this parameter on the behaviour of FRP flexural-strengthened beams. The elastic-modulus values used range from 111 GPa to 390 GPa. Fig. 12 shows the load-deflection relationships for the different values of FRP elastic modulus. A comparison between these results illustrates that the ultimate load capacity is proportional to the FRP elastic modulus. The implication of this argument is that, as the FRP becomes stiffer, a greater FRP contribution is obtained. For both beam sets considered, the load-carrying capacity tends to increase as the FRP elastic modulus increases. Therefore, with increasing FRP elastic modulus, the FRP contribution increases, and the ultimate load-carrying capacity reaches higher values, as indicated in Fig. 12. As presented in

Table 4
Various ranges of investigated parameters.

Obaidat et al. [68]						Esfahani et al. [69]				
Spec.	Parameter Variation					Parameter Variation				
	Width (mm)	Thickness (mm)	Length (mm)	E (GPa)	Layers	Width (mm)	Thickness (mm)	Length (mm)	E (GPa)	Layers
1	40	1.2	1560	165	1	40	0.176	1400	237	1
2	50	1.2	1560	165	1	50	0.176	1400	237	1
3	80	1.2	1560	165	1	80	0.176	1400	237	1
4	100	1.2	1560	165	1	100	0.176	1400	237	1
5	120	1.2	1560	165	1	120	0.176	1400	237	1
6	150	1.2	1560	165	1	150	0.176	1400	237	1
7	50	0.176	1560	165	1	150	0.330	1400	237	1
8	50	0.33	1560	165	1	150	0.501	1400	237	1
9	50	0.501	1560	165	1	150	1.000	1400	237	1
10	50	1	1560	165	1	150	1.200	1400	237	1
11	50	1.4	1560	165	1	150	1.400	1400	237	1
12	50	1.2	1960	165	1	150	0.176	2000	237	1
13	50	1.2	1040	165	1	150	0.176	933.33	237	1
14	50	1.2	520	165	1	150	0.176	466.66	237	1
15	50	1.2	1560	165	1	150	0.176	1400	237	1
16	50	1.2	1560	165	2	150	0.176	1400	237	2
17	50	1.2	1560	165	3	150	0.176	1400	237	3
18	50	1.2	1560	111	1	150	0.176	1400	111	1
19	50	1.2	1560	237	1	150	0.176	1400	165	1
20	50	1.2	1560	305	1	150	0.176	1400	305	1
21	50	1.2	1560	390	1	150	0.176	1400	390	1

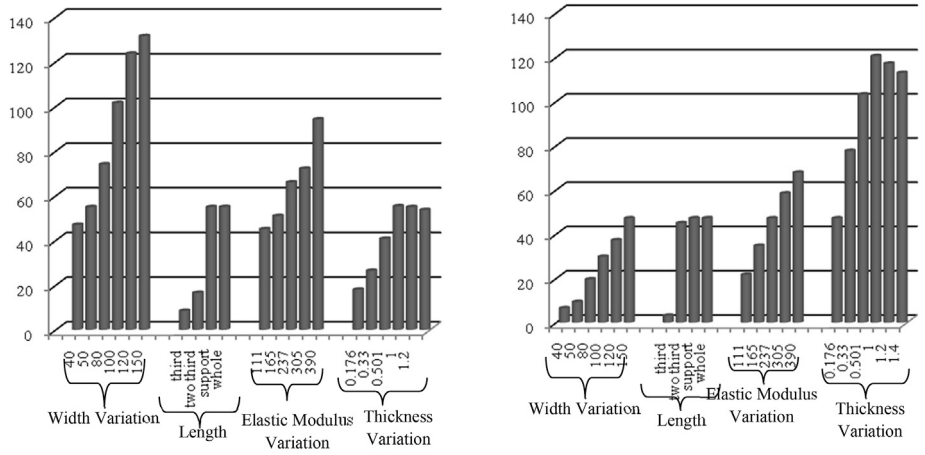

(a) Obaidat *et al.* (2011) (b) Esfahani *et al.* (2007)

Fig. 14. FRP contribution percentage for each parameter compared to control beam.

Fig. 14, the maximum increase in the FRP elastic modulus is 3.5 over the control specimen, which is identical to the percentage increase in the FRP contribution.

5.2.4. *Effect of FRP length*

This parameter has shown to have a significant effect on the ultimate load capacity of FRP flexural-strengthened beams. In the present study, the length is taken as the ratio between the FRP length and the beam span length. The ratios considered are one-third of the beam span, two-thirds of the beam span, a length covering the beam span, and a length covering the total length of the beam. For the beams described by Obaidat et al. [68]; similarly to the effect of FRP thickness, the ultimate load capacity increases with increasing FRP length 13 shows that a substantial increase in ultimate load capacity is obtained for an FRP length of two-thirds of the beam span. The contribution of the FRP sheet does not significantly change with further increase of its length. The effect of FRP length on the flexural contribution can be better visualized in Fig. 14. This can be explained as specific FRP length is required longer than the maximum moment region and cracking zone. The results obtained in this study are different from the one published by Hooque [21]; who stated that the increase of FRP length beyond 50% of the beam length does not add significant contribution to the load-carrying capacity and the mid-span deflection.

5.2.5. *Effect of number of layers*

The number of layers plays an important role in the behaviour of FRP flexural-strengthened beams. Fig. 15 shows that the stiffness increases as the number of layers is increased for both sets of specimens. Note that when a single layer, double layers, and triple layers are used for the beams described by Obaidat et al. [68]; the load capacity increases by 54.9%, 92.9% and 100.1%, respectively, compared to the control specimen. The increase in load capacity is accounted for by the increase in number of layers. For the specimens of Esfahani et al. [69]; a FRP thickness of 0.176 mm produces a 47% increase in the load capacity when a single layer is used. Increases of 77% and 82.6%, respectively, over the control specimen are reported when double and triple layers are used. The results presented here follows the ones obtained by Hooque [21].

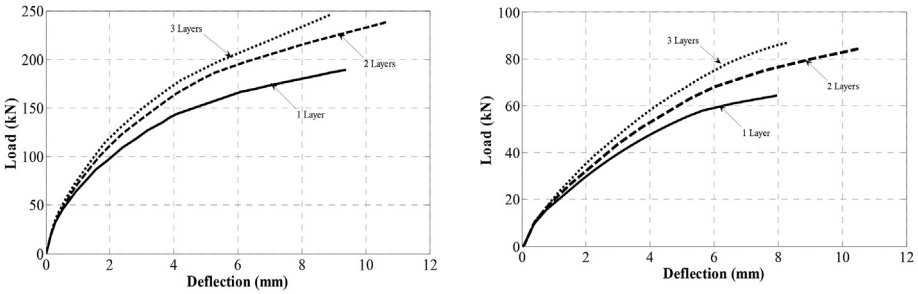

(a) Obaidat *et al.* (2011) (b) Esfahani *et al.* (2007)

Fig. 15. Effect of number of FRP layers on RC beams.

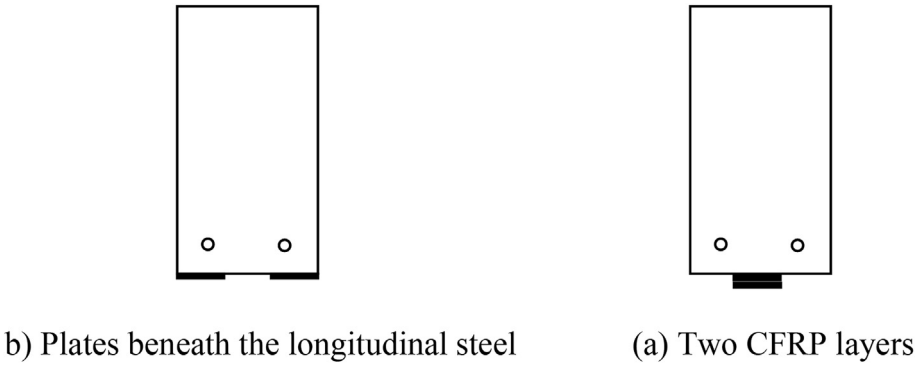

Fig. 16. Scheme of flexural-strengthening strategies.

5.2.6. Effect of FRP strengthening scheme

Fig. 16 shows the two flexural-strengthening schemes investigated in this study: FRP plates at the soffit of the beam parallel the longitudinal steel, a double layer of CFRP plates on the bottom face of the beam. In the first strengthening scheme, the gap between the plates, as well as the plate width, is 50 mm. As shown in Fig. 17, the first strengthening method, FRP plates fixed at the edges of the beam, shows a greater stiffness and increase in the load-carrying capacity than the other approach. This occurs because increasing the FRP width increases the FRP/concrete contact area. This enables a greater transfer of forces between the two adjacent surfaces and delays the debonding due to the larger contact area. For the double-layer method, the transfer of forces between the concrete and the FRP plates occurs in the central part of the beam width, whereas no attention is given to the longitudinal steel on the left and right sides of the cross section. When the CFRP plates are located on the bottom edge of the beam surface beneath the longitudinal steel, additional stresses is transferred; hence, increasing the CFRP contribution. This result confirm the findings of Jassam and Altaee [36].

6. Conclusions

A non-linear finite-element model was developed to verify the parameters that influence most the behaviour of FRP flexural-strengthened beams. The model was successfully validated using two sets of experimental results having various strengthening properties. One experimental set was pre-cracked before strengthening, which has been rarely investigated numerically in the literature. The finite element model carried out in this study used a new method of simulating the FRP/concrete interfacial behaviour. The meso-scale technique of simulating the concrete cover, where the debonding failure occurs, can predict the debonding accurately. Then, the numerical model was used to perform a parametric study to investigate the parameters having a major influence on the behaviour of FRP flexural-strengthened beams, namely: the FRP width, length, thickness, elastic modulus and number of layers. Two flexural-strengthening schemes widely used in practice were examined and compared in this study: two FRP plates at the soffit of the beam parallel the longitudinal steel, a double layer of CFRP plates on the bottom face of the beam. The results of the parametric study were

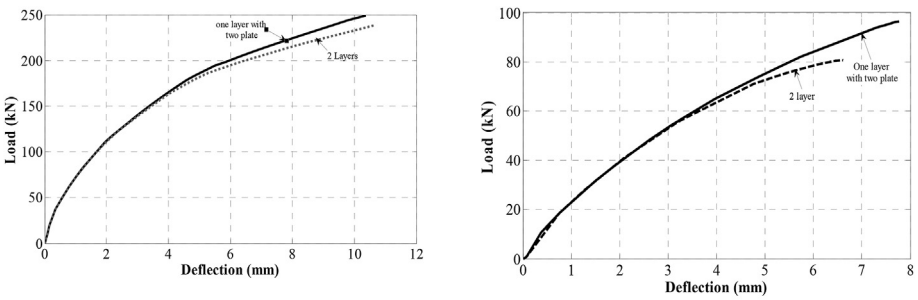

(a) Obaidat *et al.* (2011) (b) Esfahani *et al.* (2007)

Fig. 17. Load-deflection relationship for the flexural-strengthening method.

compared based on the ultimate load-carrying capacity and load-deflection relationships. On the basis of the obtained results, the following conclusions can be drawn:

- For both beam sets, the parametric study indicated that increasing the FRP width as well as the FRP elastic modulus results in proportionally related increase of FRP contribution to the load carrying capacity;
- The load carrying capacity and stiffness of strengthened beams increased as the FRP thickness was increased up to a threshold thickness of 1.0 mm. Beyond this limit, further increase in the FRP thickness did not induce any increase in the load carrying capacity;
- Similar to the effect of FRP thickness, the increase in FRP contribution is proportional to the increase of FRP length up to a certain limit. Additional increase in FRP length did not produce any significant increase in the load carrying capacity;
- The FRP contribution is affected by the strengthening scheme used for flexure. Thus, a strengthening scheme involving two FRP laminates bonded to the bottom face of the beam beneath the longitudinal steel is very effective in enhancing the FRP contribution. This method increased the bond area and delayed the debonding.

Data availability statement

All data, models, and code generated or used during the study appear in the submitted article.

Credit authors statement

The authors of this paper would like to state that:

The corresponding author is responsible for ensuring that the descriptions are accurate and agreed by all authors;
The roles of all authors is as follows: **Ahmed Godat:** Conceptualization, Methodology, Model development, Formal analysis, Investigation, Visualization, Writing- Reviewing and Editing, Funding acquisition. **Omar Chaallal:** Visualization, Writing- Reviewing and Editing. **Yasmeen Obaidat**: Formal analysis, Investigation.
Authors are contributed in multiple roles.
The role of authors does not change the journal's criteria to qualify for authorship.

Declaration of competing interest

The authors declare that they have no known competing financial interests or personal relationships that could have appeared to influence the work reported in this paper.

Acknowledgement

The authors express their appreciation to the Research Affairs Office at the United Arab Emirates University for financial support of the project under fund grant 31N375.

Nomenclature

The following symbols are used in paper.

d_c	ratio of inelastic strain to total strain
dmax	maximum aggregate size;
dt	ratio of cracking strain to the total strain
E0	concrete uniaxial elastic modulus
Ec	concrete elastic modulus
fc'	concrete compressive strength
ft	concrete tensile strength
Gf	concrete fracture energy
RE	constant taken as 4.0
Rσ	constant taken as 4.0
wc	compressive stiffness recovery
wt	tensile stiffness recovery
εc	concrete compressive strain
ε0	concrete uniaxial compressive strain
σc	concrete uniaxial compressive stress
σco	limit strength for concrete linear elastic
σcu	concrete ultimate strength

References

[1] K.W. Neale, FRPs for structural rehabilitation: a survey of recent progress, Prog. Struct. Eng. Mater. 2 (2) (2000) 133–138.
[2] B. Taljsten, FRP Strengthening of Existing Concrete Structures, first ed., Luleå University, Luleå, Sweden, 2002.
[3] H.T. Hu, F.M. Lin, Y.Y. Jan, Nonlinear finite element analysis of reinforced concrete Beams strengthened by fibre reinforced plastics, Compos. Struct. 63 (2001) 271–281.
[4] J.G. Teng, J.W. Zhang, S.T. Smith, Interfacial stresses in reinforced concrete beams bonded with a soffit plate: a finite element study, Construct. Build. Mater. 16 (2002a) 1–14.
[5] N. Pesic, K. Pilakoutas, Concrete beams with externally bonded flexural FRP reinforcement: analytical investigation of debonding failure, Compos. B Eng. 34 (2003) 327–338.
[6] Z. Yang, J. Chen, D. Proverbs, Finite element modelling of concrete cover separation failure in FRP plated RC beams, Construct. Build. Mater. 17 (1) (2003) 3–13.
[7] S. Giuseppe, Finite element analysis of RC beams retrofitted with fibre reinforced polymers. Doctoral thesis, Universit'a degli Studi di Napoli Federico II, Naples, Italy, 2005, p. 220p.
[8] L.J. Li, Y.C. Guo, F. Liu, J. Bungey, An experimental and numerical study of the effect of thickness and length of CFRP on performance of repaired reinforced concrete beams, Construct. Build. Mater. 20 (2006) 901–909.
[9] G. Camata, E. Spacone, R. Zarnic, Experimental and nonlinear finite element studies of RC beams strengthened with FRP plates, Composites Part B 38 (2) (2007) 277–288.
[10] R. Kotynia, H.M. Abdel Baky, K.W. Neale, U.A. Ebead, Flexural strengthening of RC beams with externally bonded CFRP systems: test results and 3-D nonlinear finite element analysis, Composites for Construction 12 (2) (2008) 190–201.
[11] A.M. Ibrahim, W.D. Salman, Finite element analysis of reinforced concrete beams strengthened with CFRP in flexural, Diyala Journal of Engineering Sciences 2 (2) (2009) 88–104.
[12] R. Azzawi, N. Varughese, Flexural behavior of preflex sfrc-encased steel joist composite beams, Results in Engineering 7 (2020) 100122.
[13] A.F. Ashour, S.A. El-Refaie, S.W. Garrity, Flexural strengthening of RC continuous beams using CFRP laminates, Cement Concr. Compos. 26 (2004) 765–775.
[14] H. Pham, R. Al-Mahaidi, Experimental investigation into flexural retrofitting of reinforced concrete bridge beams using FRP composites, Compos. Struct. 66 (2004) 617–625.
[15] J. Lundquist, H. Nordin, B. Täljsten, T. Olafsson, Numerical analysis of concrete beams strengthened with CFRP: a study of anchorage length, in: The International Symposium of Bond Behaviour of FRP in Structures, 2005. Hong Kong, China, 7-9 Dec., 8 pages.
[16] Z. Ai-Hui, J. Wei-Liang, L. Gui-bing, Behaviour of preloaded RC beams strengthened with CFRP laminates, Journal of Zhejiang University Science A (2006) 436–444.
[17] C.A. Coronado, M.M. Lopez, Sensitivity analysis of reinforced concrete beams strengthened with FRP laminates, Cement Concr. Compos. 28 (2006) 102–114.
[18] N. Pannirselvam, P. Raghunath, K. Suguna, Strength modeling of reinforced concrete beam with externally bonded fibre-reinforcement polymer reinforcement, Am. J. Eng. Appl. Sci. 1 (3) (2008) 192–199.
[19] M. Arduini, A. Nanni, Behavior of precracked RC beams strengthened with carbon FRP sheets, Composites for Construction 1 (2) (1997) 63–70.
[20] H. Akbarzadeh, A.A. Maghsoudi, Flexural strengthening of RC continuous beams using hybrid FRP sheets, in: The 5th International Conference on FRP Composites in Civil Engineering (CICE 2010), 27–29, 2010 (September, Beijing, China).
[21] M. Hooque, 3D Nonlinear Mixed Finite-Element Analysis of RC Beams and Plates with and without FRP Reinforcement, University of Manitoba, Winnipeg, Canada, 2006. Master Thesis.
[22] E. David, C. Djelal, F. Buyle-Bodin, Repair and strengthening of reinforced concrete beams with external composite laminates, Strength Mater. 35 (2) (2003) 128–135.
[23] H. Toutanji, L. Zhao, Y. Zhang, Flexural behavior of reinforced concrete beams externally strengthened with CFRP sheets bonded with an inorganic matrix, Eng. Struct. 28 (4) (2006) 557–566.
[24] H. Rahimi, A. Hutchinson, Concrete beams strengthened with externally bonded FRP plates, Composites for Construction 5 (1) (2001) 44–56.
[25] J. Teng, J. Chen, S. Smith, L. Lam, FRP-strengthened RC Structures, first ed., John Wiley, UK, 2002b.
[26] C.K.Y. Leung, FRP debonding from a concrete substrate: some recent findings against conventional belief, Cement Concr. Compos. 28 (2006) 742–748.
[27] A. Al-Tamimi, R. Hawileh, J. Abdalla, H. Rasheed, Effects of ratio of CFRP plate length to shear span and end anchorage on flexural behavior of SCC RC beams, Composites for Construction 15 (6) (2011) 908–919.
[28] M.K. Hind, M. Özakça, T. Ekmekyapar, A review on nonlinear finite element analysis of reinforced concrete beams retrofitted with fiber reinforced polymers, Journal of Advanced Research in Applied Mechanics 22 (1) (2016) 13–48.

[29] P. Pathak, Nonlinear Finite Element Analysis of FRP Strengthened RC Beams under Static and Cyclic Loads, Master Thesis, University of New South Wales, Canberra, Australia, 2016.
[30] Y.-S. Shin, C. Lee, Flexural behaviour of reinforced concrete beams strengthened with carbon fibre-reinforced polymer laminates at different levels of sustaining load, ACI Struct. J. 100 (2) (2003) 231–239.
[31] R. Hawileh, H. Rasheed, J. Abdalla, A. Al-Tamimi, Behavior of reinforced concrete beams strengthened with externally bonded hybrid fiber reinforced systems, Mater. Des. 53 (2014) 972–982.
[32] Z. Wu, S. Hemdan, Debonding in FRP-strengthened flexural members with different shear-span ratios, in: C.K. Shield, J. Busel, S. Walkup, D. Gremel (Eds.), The 7th International Symposium on Fibre-Reinforced Composite Reinforcement for Concrete Structures, (FRPRCS)-SP-230-24, vol. 1, ACI, Michigan, USA, 2005, pp. 411–426.
[33] P. Fanning, O. Kelly, Ultimate response of RC beams strengthened with externally bonded FRP, Composites for Construction 5 (2) (2001) 102–113.
[34] D.M. Nguyen, T.K. Chan, H.K. Cheong, Brittle failure and bond development length of CFRP-concrete beams, Composites for Construction 5 (1) (2001) 12–17.
[35] X.Z. Lu, L.P. Ye, J.G. Teng, J.J. Jiang, Mesoscale finite-element model for FRP sheets/plates bonded to concrete, Eng. Struct. 27 (4) (2005) 564–575.
[36] M. Jassam, M. Altaee, Effect of CFRP plate location on flexural behavior of RC beam strengthened with CFRP plate, in: The International Conference on Advanced Science, Engineering and Information Technology, 2011, 14 - 15 January, Putrajaya, Malaysia.
[37] S.F. Brena, R.M. Bramblett, S.L. Wood, M.E. Kreger, Increasing flexural capacity of reinforced concrete beams using carbon fibre-reinforced polymer composites, ACI Struct. J. 100 (1) (2003) 36–46.
[38] S.F. Brena, M.M. Macri, Effect of carbon fibre reinforced polymer laminate configuration on the behaviour of strengthened reinforced concrete beams, Composites for Construction 8 (3) (2004) 229–240.
[39] N. Kishi, G. Zhang, H. Mikami, Numerical cracking and debonding analysis of RC beams reinforced with FRP sheet, Composites for Construction 9 (6) (2005) 507–514.
[40] H. Niu, Z. Wu, Effects of FRP-concrete interface bond properties on the performance of RC beams strengthened in flexure with externally bonded FRP sheets, Materials in Civil Engineering 18 (5) (2006) 723–731.
[41] M.R. Aram, C. Czaderski, M. Motavalli, Debonding failure modes of flexural FRP-strengthened RC beams, Composites Part B 39 (5) (2008) 826–841.
[42] H. Abdel-Baky, Nonlinear Micromechanics-Based Finite Element Analysis of the Interfacial Behaviour of FRP-Strengthened Reinforced Concrete Beams, University of Sherbrook, Sherbrook, Canada, 2008. Ph.D. Thesis.
[43] D.S. Yang, S.K. Park, K.N. Neale, Flexural behaviour of reinforced concrete beams strengthened with prestressed carbon composites, Compos. Struct. 88 (2009) 497–508.
[44] D. Kachlakev, T. Miller, S. Yim, Finite Element Modeling of Reinforced Concrete Structures Strengthened with FRP Laminates, Oregon Department of Transportation, USA, 2001. SPR 316 Final Report.
[45] S.H. Hashemi, R. Rahgozar, A.A. Maghsoudi, Finite element and experimental serviceability analysis, Am. J. Appl. Sci. 4 (9) (2007) 725–735.
[46] M. Sundarraja, S. Rajamohan, Flexural strengthening effect on RC beams by bonded composite fabrics, J. Reinforc. Plast. Compos. 27 (14) (2008) 1497–1513.
[47] R. Balamuralikrishnan, C.A. Jeyasehar, Flexural behavior of RC beams strengthened with carbon fiber reinforced polymer (CFRP) fabrics, Open Civ. Eng. J. 3 (2009) 102–109.
[48] A. Al-Janabi, S.A. Ahmed, A.R. Safi, Behavior of RC beams strengthened with CFRP plates using the finite element modelling, in:), The 4th International Conference on FRP Composites in Civil Engineering (CICE2008, vols. 22–24, 2008. July, Zurich, Switzerland).
[49] S.L. Reddy, R. Rao, G. Rao, Evaluation of shear resistance of high strength concrete beams without web reinforcement using ANSYS, ARPN Journal of Engineering and Applied Sciences 6 (2) (2011).
[50] R. Hawileh, M. Naser, J. Abdalla, Finite element simulation of reinforced concrete beams externally strengthened with short-length CFRP plates, Composites Part B 45 (2013) 1722–1730.
[51] P. Jayajothi, R. Kumutha, K. Vijai, Finite element analysis of FRP strengthened RC beams using ANSYS, Asian Journal of Civil Engineering 14 (4) (2013) 631–642.
[52] P. Shrivastava, Y. Bajpai, A. Rai, Finite element analysis and comparative study of reinforced concrete beams laminated with and without FRP, Int. J. Eng. Sci. Res. 5 (1) (2015) 12–18.
[53] E. Choi, N. Utui, H.S. Kim, Experimental and analytical investigations on debonding of hybrid FRPs for flexural strengthening of RC beams, Composites Part B 45 (1) (2013) 248–256.
[54] M. Aktas, Y. Sumer, Nonlinear finite element analysis of damaged and strengthened reinforced concrete beams, J. Civ. Eng. Manag. 20 (2) (2014) 201–210.
[55] S.S. Zhang, J.G. Teng, Finite element analysis of end cover separation in RC beams strengthened in flexure with FRP, Eng. Struct. 75 (2014) 550–560.
[56] K. Ghaedi, Z. Ibrahim, A. Javanmardi, M. Jameel, U. Hanif, S.K. Rehman, M. Gordan, Finite element analysis of strengthened beam deliberating elasticity isotrpic CFRP material, Journal of Civil Engineering, Science and Technology 9 (2) (2018) 117–126.
[57] S. Jiang, W. Yao, J. Chen, T. Cai, Finite element modelling of FRP-strengthened RC beam under sustained load, Advances in Materials Science and Engineering (2018), 7259424.
[58] M.T. Marvila, A.R.G. Azevedo, J. Alexandre, C.M.F. Vieira, E.B. Zanelato, G.C.G. Delaqua, G.C. Xavier, S.N. Monteiro, Study of compressive strength of mortars as a function of material composition, workability, and specimen geometry, Model. Simulat. Eng. (2020) 6. ID 1676190.
[59] G.,I. Ofoegbu, B. Biswajit Dasgupta, K.J. Smart, Fracture-based mechanical modeling of concrete, Results in Engineering 7 (2020) 100107.
[60] A. Godat, K.W. Neale, P. Labossière, Numerical investigation of the parameters influencing the behaviour of FRP shear-strengthened beams, Construct. Build. Mater. 32 (2012) 90–98.
[61] Karlsson Hibbitt, Sorensen, ABAQUS Theory Manual, User Manual Example Manual, 2010 (Providence, RI), version 6.10.
[62] American Concrete Institute (ACI), Building Code Requirements for Structural Concrete and Commentary, 2014. Report No. 318-14, Farmington Hills, Michigan.
[63] American Concrete Institute (ACI), Guide for the Design and Construction of Externally Bonded FRP System for Strengthening Concrete Structures, 2014. Report No. 440 2R-14, Farmington Hills, Michigan.
[64] Comité Euro-International du Béton, CEP-FIP Model Code 1990, CEB Bulletin d'Information No. 2013, Paris, France, 1993.
[65] L. Saenz, Equation for the stress-strain curve of concrete, ACI Journal 61 (1964) 1229–1235.
[66] H.-T. Hu, W.C. Schnobrich, Constitutive modelling of concrete by using nonassociated plasticity, Materials in Civil Engineering 1 (4) (1989) 199–216.
[67] A. Wosatko, A. Genikomsou, J. Pamin, M.A. Polak, Examination of two regularized damage-plasticity models for concrete with regard to crack closing, Eng. Fract. Mech. 194 (2018) 191–211.
[68] Y.T. Obaidat, S. Heyden, O. Dahlblom, G. Abu-Farsakh, Y. Abdel-Jawad, Retrofitting of reinforced concrete beams using composite laminates, Construct. Build. Mater. 25 (2011) 591–597.
[69] M. Esfahani, M. Kianoush, A. Tajari, Flexural behaviour of reinforced concrete beams strengthened by CFRP sheets, Eng. Struct. 29 (2007) 2428–2444.